Stability Studies of FhuA, a Two-Domain Outer Membrane Protein from *Escherichia coli*†

Mélanie Bonhivers, Michel Desmadril, Gregory S. Moeck,§ Pascale Boulanger, Anne Colomer-Pallas, and Lucienne Letellier*

Institut de Biochimie et Biophysique Moléculaire et Cellulaire, UMR CNRS 8619, Université Paris Sud, Bât 430, 91 405 Orsay Cedex, France

Received July 25, 2000; Revised Manuscript Received November 9, 2000

ABSTRACT: FhuA (MM 78.9 kDa) is an *Escherichia coli* outer membrane protein that transports iron coupled to ferrichrome and is the receptor for a number of bacteriophages and protein antibiotics. Its three-dimensional structure consists of a 22-stranded β-barrel lodged in the membrane, extracellular hydrophilic loops, and a globular domain (the "cork") located within the β-barrel and occluding it. This unexpected structure raises questions about the connectivity of the different domains and their respective roles in the different functions of the protein. To address these questions, we have compared the properties of the wild-type receptor to those of a mutated FhuA (FhuA Δ) missing a large part of the cork. Differential scanning calorimetry experiments on wild-type FhuA indicated that the cork and the β-barrel behave as autonomous domains that unfold at 65 and 75 °C, respectively. Ferrichrome had a strong stabilizing effect on the loops and cork since it shifted the first transition to 71.4 °C. Removal of the cork destabilized the protein since a unique transition at 61.6 °C was observed even in the presence of ferrichrome. FhuA Δ showed an increased sensitivity to proteolysis and to denaturant agents and an impairment in phage T5 and ferrichrome binding.

Membrane-spanning proteins are classically divided into two classes according to their type of folding. The first class is constituted by proteins that adopt predominantly an α-helical structure. Such structure is mostly represented among receptors, transporters, and ion channels. Members of the second class of proteins, those that fold into β-barrels, are essentially found in the outer membrane of Gram-negative bacteria. Both classes of proteins have been the subject of numerous folding studies (for a recent review see ref *1*). Porins represent the most abundant family of β-barrel-forming proteins (*2*). A unique feature of these proteins is their high stability: they resist heat, chaotropic salts, detergents, and proteolysis. Analysis and interpretation of stability studies are strongly supported by the knowledge at high resolution of their three-dimensional structures. These studies have focused on two representative members of this family: OmpF porin, consisting of a trimer of 16-stranded β-barrels (*3*, *4*), and monomeric OmpA (*5*−*7*), the transmembrane part of which is formed by an 8-stranded β-barrel.

Another family of β-barrel proteins consists of metal chelate transporters. Although minor constituents of the outer membrane, they play an essential role in the growth and pathogenicity of Gram-negative bacteria. Most of them are multifunctional: they transport compounds structurally related to the metal chelates such as antibiotics and are receptors for phage and toxins (recently reviewed in ref *8*). They differ from porins by their high affinity and specificity for substrate and by the complexity of their function. A unique feature is that solute transport across the outer membrane, as catalyzed by these proteins, is coupled to the electrochemical gradient of protons in the cytoplasmic membrane via the cytoplasmic membrane-anchored protein complex TonB−ExbB−ExbD (for a recent review see ref *9*). The recent determination of the three-dimensional structure at 2.5 Å resolution of two *Escherichia coli* iron-chelate (siderophore) transporters, FhuA (*10*, *11*) and FepA (*12*), has revealed an unexpected feature of this family of proteins. The ferrichrome transporter FhuA is composed of a barrel domain consisting of 22 antiparallel β-strands (residues 161−714) lodged in the membrane and of an amino-terminal globular domain (residues 1−160) that folds inside the barrel and occludes it. This "plug" (*11*) or "cork" (*10*) domain, which spans most of the interior of the β-barrel, consists of a four-stranded β-sheet and four short helices that are connected to the β-barrel and to hydrophilic loops facing the external medium and involved in ligand binding. Interestingly, residues located at three of the apexes of the cork domain play a critical role in ligand binding. Few structural changes are observed in the cork domain upon ligand binding, with one notable exception. A helix (residues 24−29; the "switch helix") located in the periplasmic pocket in the ligand-free conformation of FhuA is completely unwound upon ferrichrome binding.

In vivo studies based on mutations deletions and insertions have highlighted the contributions of various regions of FhuA

† G.S.M. acknowledges fellowship support from the Ministère des Affaires Étrangères, France, and from the Natural Sciences and Engineering Research Council, Canada.

* To whom correspondence should be addressed. L. Letellier, E-mail: lucienne.letellier@biomemb.u-psud.fr. Telephone: (+33) 1 69 15 64 29. Fax: (+33) 1 69 85 37 15.

§ Present address: Phage Tech, Inc., C. P. 387, Place du Parc, Montréal, Québec, Canada, H2W 2N9.

10.1021/bi001725i CCC: $20.00
Published on Web 02/02/2001

in its functions. In particular, Carmel and Coulton (*13*) demonstrated that a mutated FhuA (FhuA Δ021−128),[1] missing a large portion of the cork, retained function since an *E. coli* strain expressing FhuA Δ showed growth promotion by ferri-ferrichrome and plating efficiencies for phages T1, T5, UC-1, and ϕ80 equivalent to those of wild-type FhuA. More recently, Braun et al (*14*) showed that FhuA Δ5−160, which lacks the whole cork domain, displayed in vivo functionality. Interestingly, some shorter deletions within the cork strongly reduced in vivo activity (*13*) or led to degraded proteins (*14*), suggesting complex interrelationships between the different domains of FhuA.

This complex and very unusual structure of FhuA raises the question of the connectivities of the β-barrel and cork domains. Do they behave as autonomous folding domains? How does the cork domain contribute to the stability of the protein? To address these questions, we took advantage of the availability of a recombinant FhuA Δ021−128 (referred as FhuA Δ). The protein, which carries a hexahistidine tag, is functional in vivo (*15*) and can be purified in a stable form. FhuA also offers a sensitive, specific, and quantitative functional assay in vitro: a fluorescence-based measurement of DNA release from phage T5 upon its binding to the purified receptor (*16*).

In this work, we have performed in vitro functional assays and denaturation experiments on FhuA WT and FhuA Δ and compared the effects of ligand binding on their stability. To probe the behavior of the proteins under various conditions of heat and chemical denaturants, we used immunochemical and biophysical assays. It is concluded that the β-barrel behaves as an independent folding domain and that both the cork and the loops contribute to the stability of FhuA.

MATERIALS AND METHODS

Overexpression and Purification of FhuA WT and FhuA Δ. *E. coli* strain HO830*fhuA* was transformed with plasmids pHX405 (*17*) and pCG405 (*15*) and used for overexpression of FhuA WT and FhuA Δ, respectively. The recombinant proteins carried a hexahistidine tag inserted after amino acid 405 and five additional linker residues. Proteins were purified according to ref *17* with slight modifications. Cells were grown overnight at 37 °C in LB medium and in the presence of 100 μM dipyridyl and 125 μg/mL ampicillin. Outer membrane vesicles were prepared by lysozyme-EDTA treatment and solubilized in 0.5% LDAO (w/w). They were dialyzed extensively against 50 mM Tris-HCl, pH 8.0, 150 mM NaCl, 0.5% LDAO, 1 mM NaN_3 prior to batch-incubation with Ni^{2+}-NTA resin (Qiagen). Typically, an extract from 14 g of wet cells was loaded onto 5 mL of packed resin. Proteins were eluted with 50 mM Tris-HCl, pH 8.0, 150 mM NaCl, 0.1% LDAO, 500 mM imidazole and dialyzed against 50 mM Tris-HCl, pH 8.0, 150 mM NaCl, 0.05% LDAO, 1 mM NaN_3 (TLN buffer). Purified proteins were concentrated by ultrafiltration and stored at −20 °C.

[1] Abbreviations: CD: circular dichroism; DSC: differential scanning calorimetry; FhuA Δ: FhuA Δ021−128; LB: Luria broth; LDAO: *n*,*n*-dimethyldodecylamine *n*-oxide; PAGE: polyacrylamide gel electrophoresis; PVDF: polyvinylidene fluoride; SDS: sodium dodecyl sulfate; TLN buffer: 50 mM Tris-HCl, pH 8.0, 150 mM NaCl, 0.05% LDAO, 1 mM NaN_3; TPCK: L-1-tosylamido-2-phenylethyl chloromethyl ketone; YO-PRO-1: quinolinium,4-[(3-methyl-2(3H)-benzoxalydene)-methyl]-1-[3(trimethylammonio)propyl1]-, diiodide.

Fluorescence Assay of phage T5 Binding and DNA Release. Experiments were carried out according to Boulanger et al (*16*) except that ferrichrome was loaded with Fe^{3+}. Briefly, given concentrations of FhuA WT or FhuA Δ were added to 1 mL of TLN buffer containing 4 μM YO-PRO-1 (Molecular Probes) and incubated at 37 °C for 5 min. Phage T5 (2×10^9 phage/mL) was then added, and the kinetic of DNA release was monitored by measuring the increase of fluorescence emission intensity with time (λ_{ex} = 490 nm, λ_{em} = 509 nm) on an SLM8000 spectrofluorimeter. Competition experiments were carried out by adding variable concentrations of ferri-ferrichrome prior to addition of the phage. Phage stocks (1×10^{12} phage/mL in 10 mM Tris, pH 7.5, 150 mM NaCl, 1 mM $CaCl_2$, 1 mM $MgSO_4$) were prepared according to ref *18*.

FhuA Receptor Activity as Determined from the Plaque Inhibition Assay. Receptor activity was determined according to ref *16*. Briefly, phage T5 (4×10^6 particles) was incubated at 37 °C with given concentrations of FhuA WT or FhuA Δ in TLN buffer. The protein molecules to T5 phage particles ratio was varied from 10^7 to 10^{11}. After 30 min, aliquots were rapidly diluted (1000-fold), mixed with *E. coli* F cells, and plated. Unbound phages were quantified from the infectious centers and compared to a control treated identically but not containing the proteins.

Determination of the K_D of Ferrichrome Binding by Equilibrium Dialysis. Equilibrium dialysis experiments were performed at room temperature with a Dianorm dialysis apparatus equipped with 5 two-compartment cells (50 μL) separated by a dialysis membrane (molecular weight cutoff 20 500). Stock solutions of 20 μM ^{55}Fe-ferrichrome were prepared by mixing in the following order: 45 μL of HCl 0.5 N, 1.9 μL $^{55}FeCl_3$ 5.65 mM (6.3×10^{13} Bq/mol), 77 μL of ferrichrome 260 μM and 376 μL of TLN buffer. Fifty microliters of ^{55}Fe-ferrichrome stock solutions of known concentrations was added to one compartment and 50 μL of the protein (100 nM of FhuA WT and up to 10 μM of FhuA Δ) was added to the other one. After overnight dialysis, the content of each compartment was recovered and 35 μL samples were counted for radioactivity. Experimental data were fitted to the standard equation with Sigma Plot and then treated using the Scatchard representation.

Electrophoresis and Immunoblotting. Samples were separated by SDS−PAGE and stained with Coomassie Brilliant Blue or transferred to PVDF membranes (Bio-Rad) for 45 min at 80 V. Membranes were incubated with primary antibodies anti-H_6 (Sigma-Aldrich), Fhu7.3, or Fhu8.1 (*19*), followed by secondary anti-mouse antibodies conjugated to horseradish peroxidase (Santa Cruz). Bands were visualized by chemiluminescence (NEN Renaissance).

For heat and SDS treatment, 2 μg of the proteins were incubated for 5 min at the indicated temperatures in the absence or presence of 2% (final concentration) SDS and without 2-mercaptoethanol in the loading buffer. Samples were then resolved on 7.5% PAGE gels. Electrophoresis was performed at 4 °C.

Trypsin Proteolysis and N-Terminal Sequencing. Digestions were performed according to Moeck et al. (*17*). Briefly, 1 μg of FhuA WT or FhuA Δ was proteolyzed by 1 μg of trypsin (TPCK treated, Sigma) in the presence or absence of 0.5 μg of ferri-ferrichrome for various times and in 50 mM Tris-HCl, pH 8.0, 0.05% LDAO. All samples were

prepared on ice before trypsin addition and then incubated at 37 °C. Reactions were stopped at given times by adding equal volumes of 2× loading buffer (containing 2.5% SDS and 10% 2-mercaptoethanol) and boiling for 3 min before loading onto SDS−10% PAGE gels. For N-terminus sequencing, 2 nmol of FhuA Δ were digested by 0.2 nmol of trypsin for 2 h at 37 °C in 10 mM Tris-HCl, pH 8.0, 0.05% LDAO. The reaction was stopped by adding 5% (final concentration) protein sequencing grade trifluoroacetic acid (Merck). The sample was then resolved on SDS−10% PAGE gels, and the band was transferred to PVDF membranes and excised. The N-terminus was sequenced using Edman degradation reaction (Applied Biosystem 473 microsequencer).

Differential Scanning Calorimetry. DSC was carried out using a MicroCal model MC2. Scans were performed at a rate of 1 K/min for temperatures ranging from 20 to 90 °C. To avoid the important variations of the pH of Tris-buffered solutions with temperature, 1 mL of each sample (FhuA WT, 0.4 mg/mL; FhuA Δ, 0.55 mg/mL) was extensively dialyzed against 100 mM sodium phosphate buffer, pH 7.2, 0.03% LDAO and thoroughly degassed before recording spectra. The same buffer was used as reference for the measurements. Scanning was performed in the presence or absence of 125 μg of ferri-ferrichrome. Every measurement was preceded by a baseline scan with buffer only or buffer plus ferri-ferrichrome. Before analysis, the heat capacity of the solvent was subtracted from that of the protein sample. Thermodynamic parameters were obtained by fitting the data to standard equations.

Circular Dichroism of FhuA WT. The melting curve of FhuA WT was monitored by circular dichroism on a Mark VI (Jobin-Yvon) dichrograph. CD spectra were collected at a protein concentration of 1 mg/mL in the same buffer as for the DSC experiments. Spectra were recorded between 190 and 250 nm at various temperatures after heating (1 K/min) and equilibration. The cell (path length 0.1 mm) as well as the cell holder were thermostated by a circulating bath and temperature was monitored directly in the cell by using a micro temperature sensor.

RESULTS

Phage T5 and Ferrichrome Binding to FhuA WT and FhuA Δ. In vivo assays have shown that FhuA Δ is functional with regards to ferrichrome transport and phage T5 binding (*13*). However, these studies did not allow for assessment of whether the deletion affected binding affinity for the ligands. To address this question, we used the fluorescent DNA intercalator YO-PRO-1, the fluorescence of which increases upon binding of phage T5 to isolated FhuA and release of its DNA into the surrounding medium (*16*). Figure 1 shows typical curves obtained upon interaction of phage T5 with purified FhuA WT and FhuA Δ. The fluorescence first increased with time, but at a rate different for each protein, and then reached the same steady-state intensity. The amount of DNA released was determined from the steady-state intensity. Calibration curves with known amounts of free DNA (data not shown) (*16*) indicated that FhuA Δ was as efficient as FhuA WT to promote phage DNA ejection since 90% of the DNA was released. In contrast, each protein behaved differently with regard to phage binding, as seen upon measurement of the initial rate of fluorescence increase (V_i) as a function of protein concentration (Figure 2, panel A). The minimum concentration of the receptor that was required to observe DNA release was 0.4 nM for FhuA WT

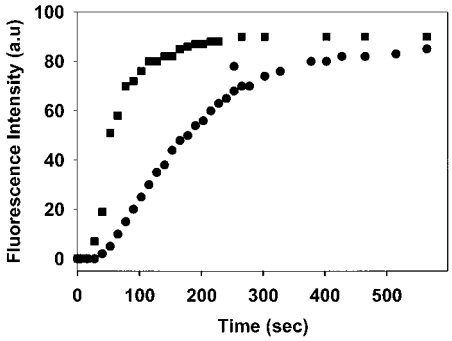

FIGURE 1: Binding of Phage T5 to FhuA WT and to FhuA Δ021−128 triggers the release of phage DNA. Purified FhuA WT (■) or FhuA Δ021−128 (●) (40 and 180 nM, final concentrations, respectively) were incubated at 37 °C in a cuvette containing 4 μM YO-PRO-1 in TLN buffer. T5 (2×10^9 phage/mL) was then added and DNA release was measured as a function of time by the increase of fluorescence emission at 509 nm ($\lambda_{ext} = 491$ nm). The fluorescence intensity was calibrated with known amounts of free DNA as described in Boulanger et al. (*16*). The plateau value corresponded in all cases to 90 ± 8% DNA released.

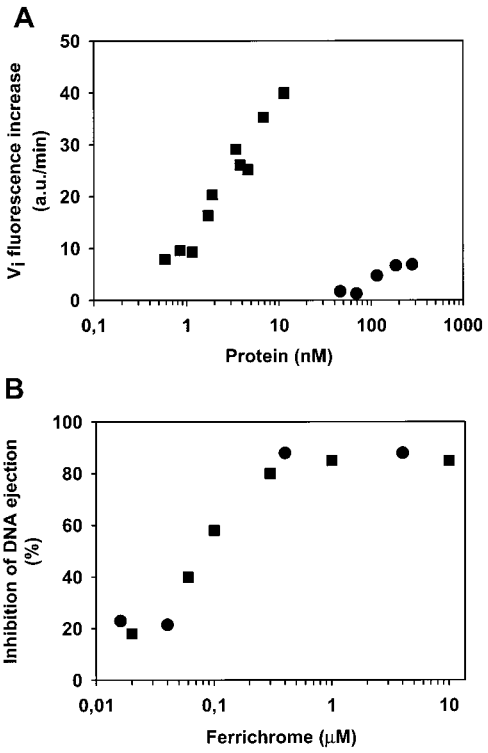

FIGURE 2: (A) Effect of FhuA WT and FhuA Δ concentration on the initial rate of fluorescence increase: conditions were as described in the legend to Figure 1 except for the concentration of the proteins [FhuA WT (■) or FhuA Δ021−128 (●)], which was varied as indicated. (B) Effect of ferri-ferrichrome concentration on the amount of phage T5 DNA released: Variable concentrations of ferri-ferrichrome were added to the cuvette containing YO-PRO-1 (4 μM) and the protein (40 and 180 nM for FhuA WT (■) and FhuA Δ (●), respectively). Phage T5 (2×10^9 phage/mL) was then added. The fluorescence increase of YO-PRO-1, induced by ejection of the DNA, was measured at 37 °C as a function of time. The percentage of inhibition of DNA release was calculated from the fluorescence at steady state. 0% of inhibition is defined as the steady-state value of the fluorescence in the absence of ferrichrome (see Figure 1).

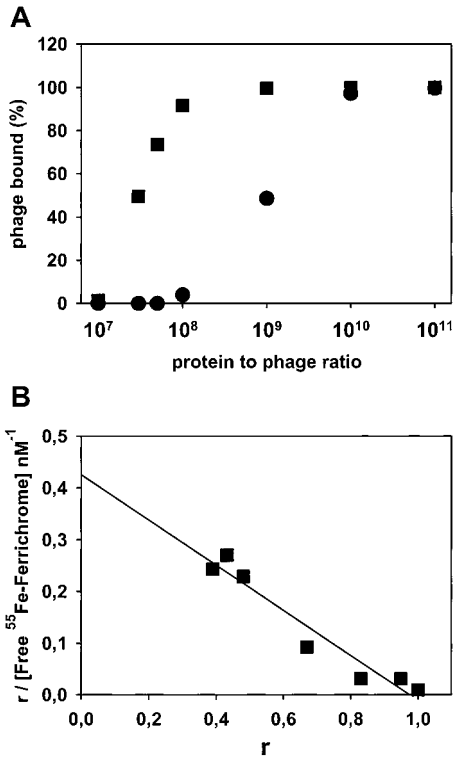

FIGURE 3: Ligand binding to FhuA WT and FhuA Δ. (A) Binding of phage T5 to FhuA WT and FhuA Δ. T5 phages (4×10^6 particles) were mixed with purified FhuA WT (■) or FhuA Δ (●) at different protein molecules/phage particle ratio. The percentage of phage bound to the proteins was deduced from a plaque inhibition assay as described in Material and Methods. **(**B) Binding of ferri-ferrichrome to FhuA WT as determined by equilibrium dialysis. Scatchard representation from fitted data where *r* represents the fraction of liganded protein.

and 40 nM for FhuA Δ. Furthermore, the maximum value of V_i obtained with FhuA Δ was four times smaller than that reached with FhuA WT. To account for these differences, T5 binding was measured using a plaque inhibition assay. Figure 3, panel A, shows that the efficiency of phage T5 binding was at least 33-fold less for FhuA Δ than FhuAWT.

Such decrease in affinity of binding was also observed for ferri-ferrichrome. Equilibrium dialysis experiments (Figure 3, panel B) allowed us to calculate a K_d of ferri-ferrichrome binding to FhuA WT of 2.1 ± 0.5 nM. Binding of ferri-ferrichrome to FhuA Δ was not detectable even when concentrations of ferri-ferrichrome up to 30 μM were used.

Surprisingly, phage T5 DNA ejection was prevented when ferri-ferrichrome was added to both proteins and before the phage. Furthermore, the concentration of ferrichrome that prevented phage T5 DNA ejection was the same (1 μM) for FhuA WT and FhuA Δ (Figure 2, panel B). The specificity of this inhibition was attested by the fact that siderophores analogues belonging to the hydroxamate family did not prevent DNA ejection at concentrations up to 1 mM (unpublished data).

Ferrichrome Does Not Protect FhuA Δ from Proteolysis. Trypsin proteolysis of FhuA WT has been shown to produce a truncated protein at Lys67 (ref *17* and Figure 4). However, ferrichrome protected FhuA WT from cleavage at this position. The trypsin sensitivity of FhuA Δ was evaluated. Two major products of FhuA Δ appeared within 5 min of

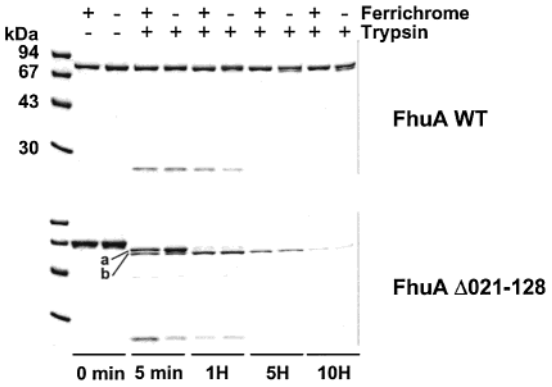

FIGURE 4: Trypsin proteolysis kinetics. FhuA WT or FhuA Δ (1 μg) were digested with 1 μg of trypsin for the indicated times in the presence (+) or absence (−) of ferri-ferrichrome (0.5 μg; corresponding to ~50-fold molar excess), and the products were resolved on SDS 10%−PAGE gels. Molecular mass markers are indicated on the left.

incubation with trypsin (Figure 4, bands a and b), whereas FhuA WT remained protected for at least 1 h. Furthermore, proteolysis of FhuA Δ was not prevented even when a 50-fold molar excess of ferri-ferrichrome was added.

To determine the site of cleavage of FhuA Δ that resulted in the appearance of the first product, the N-terminus of band a was sequenced. The trypsin cleavage occurred at the FhuA WT corresponding lysine 154 indicating that the part of the cork remaining in FhuA Δ was fully cleaved.

Effect of Heat and Chemical Denaturants on the Stability of FhuA WT and FhuA Δ. A common feature of β-barrel proteins is that nonheated samples display anomalous electrophoretic mobility. This is due to their high content of compact β-strands that bind less SDS than do other proteins so that they retain a partially folded structure (*20*, *21*). This anomalous behavior was also observed for nonheated FhuA which migrates at ca. 45 kDa (*22*). Figure 5, panel A shows that the mobility in PAGE of FhuAWT and FhuA Δ was different. FhuA WT displayed two mobilities in the absence of SDS in the loading buffer. For temperatures ranging from 4 to 60 °C, FhuA WT migrated at ca. 45 kDa. Above 60 °C and up to 100 °C, FhuA WT migrated with a relative mobility close to that calculated from the amino acid sequence (80.2 kDa) suggesting that it becomes denaturated above 60 °C. Treatment of FhuA WT with SDS shifted the transition to the denaturated state down to 40 °C. Interestingly, FhuA Δ migrated with a relative mobility (ca. 67 kDa) close to that of the denaturated form (calculated MM 68.4 kDa) at all temperatures between 4 and 100 °C, regardless of whether samples were treated with SDS.

To confirm their differences in thermal and chemical stability, FhuA WT and FhuA Δ were probed by monoclonal antibodies (Figure 5, panel B). Anti-H6 antibody, whose determinant lies in an externally facing loop (*17*, *10*), bound to both proteins under all conditions (not shown). Fhu7.3, whose determinant lies between amino acids 151 to 199 (and therefore includes part of the cork and/or of the β-barrel) and which binds the unfolded form of FhuA WT (*19*), bound the highest molecular mass band of FhuA WT as well as the single band of FhuA Δ. Fhu8.1, whose determinant lies between residues 417−550 (part of the barrel) (*19*) and which binds the folded form of FhuA, detected the lower mass band of FhuA WT but not FhuA Δ. These results confirm that

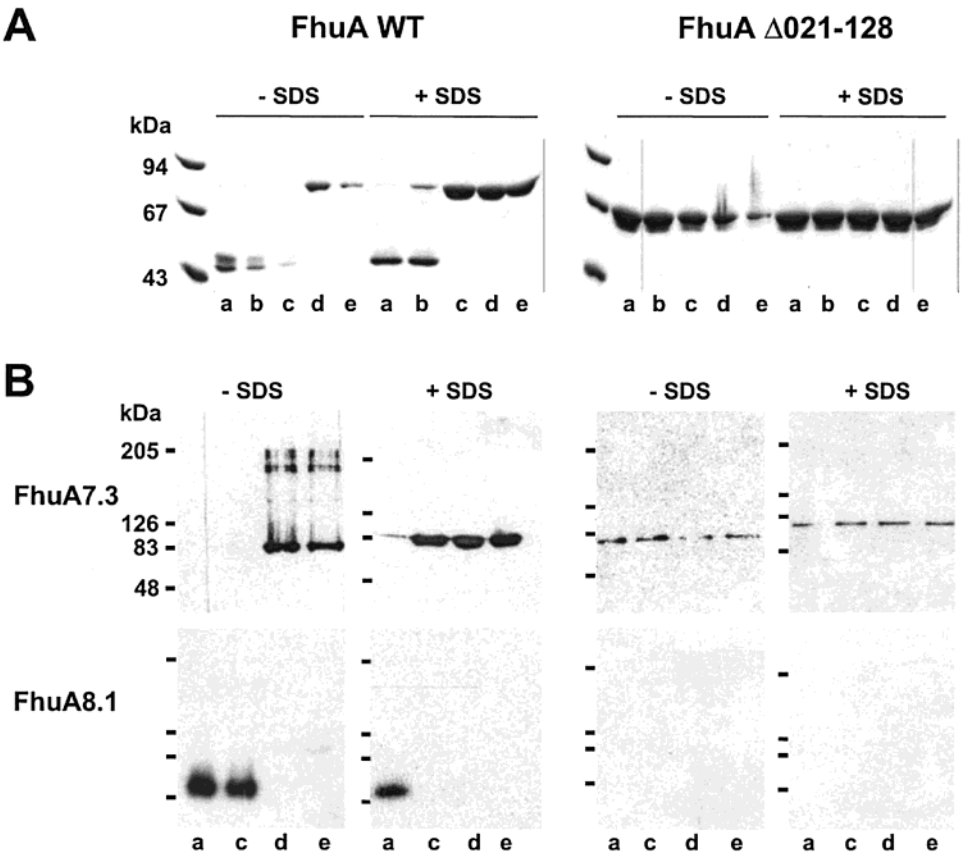

FIGURE 5: Electrophoresis and immunoblot analysis of samples heated under native and denaturing conditions. FhuA WT or FhuA Δ (2 μg) were heated at different temperatures (*a* = 4 °C, *b* = 40 °C, *c* = 60 °C, *d* = 80 °C, *e* = 100 °C) for 5 min in loading buffer containing (+) or not (−) 2% SDS and loaded on 7.5% SDS−PAGE. Molecular mass markers are indicated on the left. (A) Coomassie Blue stained gels of FhuA WT (left panel) and FhuA Δ (right panel). Some aggregation at and above 60 °C likely occurred, explaining the decrease of protein staining. (B) Corresponding immunoblots probed with primary antibodies Fhu7.3 and Fhu8.1.

FhuA WT can adopt at least two conformations, folded and unfolded, the transition between the two conformations taking place close to 60 °C in the absence of SDS and near 40 °C in the presence of SDS. In contrast, FhuA Δ adopts only the unfolded form, the presence of SDS uniquely in the running buffer being sufficient to denaturate the protein.

Changes in the Specific Heat Capacity of FhuA WT and FhuA Δ. DSC was used to characterize the unfolding process of FhuA WT and FhuA Δ and to investigate the effect of ferrichrome binding on the stability of each protein. FhuA WT free of ligand displayed two transitions centered at T_1 = 65 °C and T_2 = 74.4 °C, associated with an enthalpy of 598 and 670 kJ/mol, respectively (Figure 6, panel A). In the presence of ferri-ferrichrome, T_1 was shifted up to 71.4 °C, whereas T_2 remained unchanged. Control experiments showed that ferrichrome alone did not contribute to any signal between 50 to 90 °C (data not shown). Interestingly, FhuA Δ displayed only a single broad transition at 61.6 °C associated with an enthalpy of 836 kJ/mol whether ferrichrome was present or not (Figure 6, panel B).

FhuA WT was submitted to a temperature shift from 20 to 65 °C and then slowly cooled to 37°. The heated sample bound phage T5 and induced the release of the phage DNA with the same kinetics and efficiency as the unheated sample (data not shown) suggesting reversibility of the first transition. On the other hand activity could not be retrieved if the sample was first heated to 74 °C and then cooled to 37 °C. Functionality of FhuA Δ could not be retrieved by heating the sample to 65 °C and cooling it to 37 °C.

Thermal Denaturation of FhuA WT Monitored by Circular Dichroism. To assign the transitions observed by DSC to the different domains of FhuA WT, we performed circular dichroism measurements at variable temperatures (Figure 6, panel C). At room temperature, the far UV CD spectrum of FhuA WT is typical of an all β-protein (*16*). For temperatures up to 70 °C, there was no significant change in the ellipticity values at 193 nm indicating that the overall content in β-structure was retained. Only small changes in ellipticity at 215 nm (Figure 6, panel C, inset) were observed. For temperatures varying between 70 and 75 °C, there was a sharp decrease in ellipticity. This transition, which was superimposable to the second transition observed by DSC, led to the loss of almost all the secondary structure of the protein.

DISCUSSION

FhuA shows a very unusual fold with two distinct domains, an external 22-stranded β-barrel and an inner domain, which plugs the inner part of the barrel. The experiments described in this work show that the cork domain plays an essential role in the stability of the protein. This was demonstrated by comparing the functional and structural properties of FhuA WT to those of a mutated FhuA (FhuA Δ021−128) that lacks almost all the cork domain. Previous in vivo studies had shown that FhuA Δ could bind phage T5 and transport ferrichrome (*13*, *15*) indicating that the mutated protein was targeted to the *E. coli* outer membrane and folded so as to retain functionality. We demonstrate here that FhuA Δ

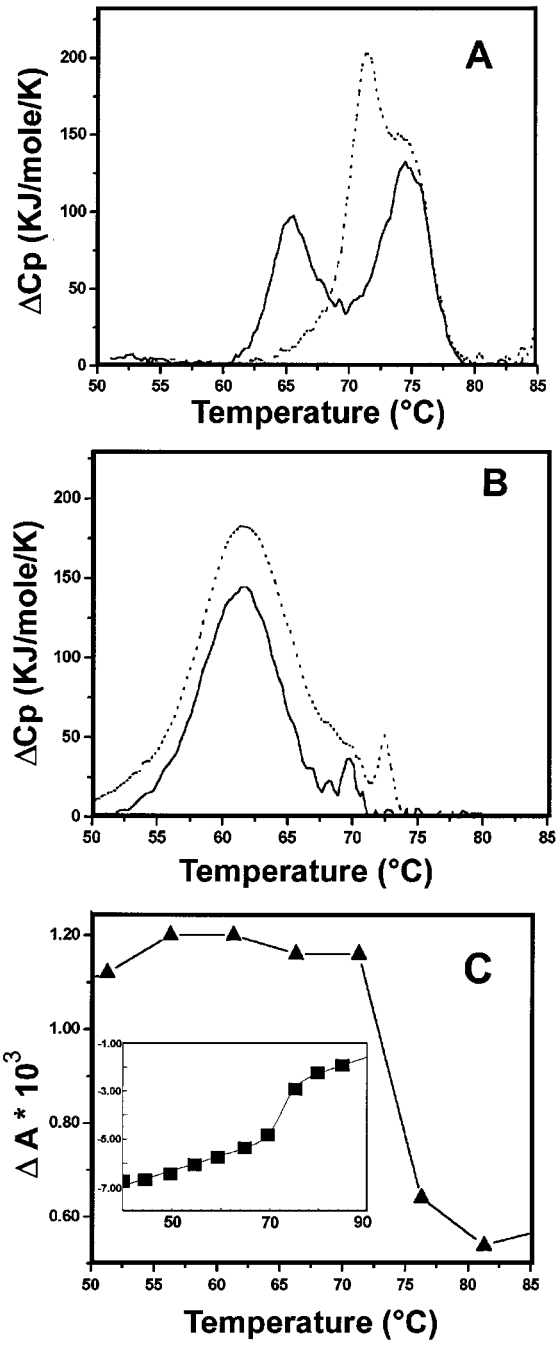

FIGURE 6: Differential Scanning Calorimetry of FhuA WT (A) and FhuA Δ (B). Samples (FhuA WT: 0.4 mg/mL; FhuA Δ: 0.55 mg/mL) were subjected to temperature increases at a rate of 1 K/min. Denaturation scans were measured in the presence (dotted line) or in the absence (solid line) of 125 μg ferri-ferrichrome. (C) Thermal stability of FhuA WT monitored by the change in ellipticity at 193 nm. Δ*A* was determined at the indicated temperatures. FhuA WT (1 mg/mL) was subjected to temperature step increases of 1 K/min. Inset: ellipticity at 215 nm.

behaves differently from FhuA WT with regard to phage T5 binding and DNA release in vitro. For DNA to be released, the phage first has to bind to FhuA. This collisional step is followed by large conformational changes in the receptor since FhuA is converted into an open channel (*18*). Simultaneously, conformational changes take place at the tip of the phage tail which are transmitted to the capsid, leading to its opening and to DNA release (*23*−*25*). We previously showed that the initial rate of increase of the fluorescence of the DNA intercalator YO-PRO-1 (V_i) reflects two different limiting steps of the DNA release process (*16*). Phage binding to FhuA is the limiting step as long as V_i depends on FhuA concentration. When V_i reaches a value independent of the receptor concentration, the limiting step becomes the conformational changes in the phage−FhuA complex that trigger DNA release. We observed that release of DNA required concentrations of FhuA Δ two orders of magnitude higher than those required for FhuA WT suggesting that removal of the cork affects phage T5 binding. This conclusion was corroborated by plaque inhibition assays that showed a 33-fold reduction in the efficiency of phage T5 binding to FhuA Δ as compared to FhuA WT. The T5 binding site was mapped (*26*) to a proposed hydrophilic loop of FhuA facing the external medium in whole cells (*27*). The connectivities between the loop and the cork are therefore important for the phage receptor activity of FhuA. Interestingly, the maximum value of the V_i of fluorescence increase measured with FhuA Δ was four times smaller than that observed with FhuA WT. This suggests that removal of the cork also affects the conformation of the phage−FhuA complex.

Removal of the cork also strongly decreased the affinity of ferri-ferrichrome for the protein. From equilibrium dialysis experiments, we determined a K_d of ferri-ferrichrome binding to FhuA WT of 2.1 nM. In contrast, the binding of ferrichrome to FhuA Δ was not detectable even when concentrations of ferrichrome up to 30 μM were used. These results are in accordance with the fact that residues belonging to the binding site of the ferrichrome are deleted in FhuA Δ (*10, 11*).

Surprinsingly, we found that phage DNA release was inhibited by addition of 1 μM ferrichrome to FhuA WT and FhuA Δ. The crystal structure of FhuA WT revealed that none of the residues of the T5 binding site contributes directly to the binding of ferrichrome and that only minor conformational changes take place in the extracellular regions upon ferrichrome binding (*11*, *10*). Braun et al. (*14*) also showed that ferrichrome did not inhibit in vivo binding of phage T5 to a mutated FhuA (FhuA Δ5−160) missing the cork. It is therefore likely that binding of phage T5 to both proteins can take place in the presence of ferrichrome. To account for the inhibition of phage DNA release, we have to postulate that phage binding triggers a conformational change in both proteins that unmasks a low affinity binding site for ferrichrome. Binding of ferrichrome would then prevent further conformational changes that lead to DNA release from phage T5. This proposal is compatible with data showing that ferrichrome at a concentration of 10 μM inhibits T5-induced channel formation in FhuA (*18*).

Studies of the effects of proteases, denaturants, and temperature gave strong indications of the reduced stability of FhuA Δ as compared to FhuA WT. Indeed, the part of the cork remaining in FhuA Δ was fully cleaved by trypsin within 5 min, whereas FhuA WT remained protected from cleavage for at least 1 h. Furthermore, and in contrast to FhuA WT, FhuA Δ was not protected from proteolysis by ferrichrome. According to the 3D structure, four residues of the FhuA WT cork (R81, Q100, F115, and Y116) that are absent in FhuA Δ may form hydrogen bonds and van der Waals contacts with ferrichrome. It is thus likely that the ferrichrome-mediated protection of FhuA Δ from trypsinolysis is lost due to deletions in the cork domain. The two

proteins also showed a different pattern of migration on PAGE and of accessibility to antibodies. FhuA WT remained folded up to 60 °C, whereas FhuA Δ was denaturated at all temperatures studied between 4 and 100 °C. The pattern of thermal denaturation of FhuA WT obtained by DSC was indicative of the presence of two well-resolved structural domains. Two transitions were observed: a first one at 65 °C which is in line with the transition temperature observed in PAGE and a second one at 75 °C. Several arguments suggest that the second transition may be assigned to the unfolding of the β-barrel. (i) An approximate calculation indicates that this transition contributes to 53% of the total enthalpy of denaturation and thus corresponds in first approximation to 53% of the total residues of the protein. This value is in agreement with the percentage of total residues (48%) constituting the β-barrel. (ii) Denaturation of the β-structure was observed at 75 °C in CD. (iii) This transition temperature is also in rather good agreement with the FTIR data of Moeck et al. (*17*) who observed a sharp decrease in the β-sheet structure of FhuA WT between 69 and 73 °C. (iv) This transition takes place at a temperature close to that determined for the denaturation of the 16 antiparallel β-stranded OmpF barrel (72 °C) (*4*). Is unfolding of the cork responsible for the first transition? The cork domain comprises 22.4% of the protein residues and contains less than 6% of the total β-sheets and only four short helices. Consistent with this composition are the absence of significant changes of ellipticity at 193 nm and the small changes measured at 215 nm for temperature up to 70 °C. Since the first transition corresponded to 47% of the total transition enthalpy, it cannot be attributed solely to the cork unfolding. Solvent exposure accompanying cork denaturation as well as the unfolding of external loops should significantly contribute to this enthalpy. Importantly, the transition was shifted from 65 to 71.4 °C by addition of ferri-ferrichrome, thus demonstrating the strong stabilizing effect of the ligand on the loops and cork. This observation is to be compared to the enterobactin-mediated stabilization of FepA in strong denaturants (*28*). Interestingly, functionality of the protein (i.e., its capacity to bind phage T5 and to trigger DNA release) was retrieved after a temperature shift to 65 °C followed by cooling to 37 °C. This result suggests reversibility of the unfolding transition for the loops and cork. Functionality was however lost upon denaturation of the β-barrel. DSC experiments further proved the lower stability of FhuA Δ as compared to FhuA WT and demonstrated the inefficiency of ferrichrome in stabilizing the protein. Indeed, a unique thermal transition was observed for FhuA Δ. Its temperature (61.6 °C) was lower than that measured for wild-type FhuA WT and was not raised by addition of ferrichrome. The four-stranded β-sheet and the four short helices forming the cork are connected to the β-barrel and to the hydrophilic loops by nine salt bridges and 60 hydrogen bonds (*10*, *11*). Given the data obtained on FhuA Δ, it is likely that they contribute significantly to the stability of the β-barrel.

There are numerous examples of soluble, multidomain proteins in which each structural domain behaves as an independent folding unit (*29*−*34*). This work is one of the first examples suggesting that in membrane proteins made of several structural domains, each domain can also behave as an autonomous folding unit. We are far from understanding how ligands are transported through metal-chelate transporters. The crystal structures of FhuA and FepA in the absence and presence of siderophores do not yet describe the changes in the receptor that must be induced during energy coupling and ligand transport, nor does the 3D structure account for the appearance of a large water-filled channel in FhuA upon phage T5 binding (*18*). We therefore still depend on indirect but also dynamic approaches. Several mutated proteins have been constructed based on the FhuA 3D structure. By combining in vivo experiments (*14*) and in vitro biophysical studies, we expect to answer, at least partially, these outstanding questions.

ACKNOWLEDGMENT

The authors thank J. W. Coulton for FhuA plasmids, Z. Amiar for technical assistance, and P. Decottignies for peptide sequencing. We are indebted to A. Sansom for access to the CD apparatus. We thank F. Pattus as well as I. Schalk and D. Massotte for support in equilibrium dialysis experiments.

REFERENCES

1. Booth, P. J., and Curran, A. R. (1999) *Curr. Opin. Struct. Biol. 9*, 115−21.
2. Nikaido, H., and Saier, M. H. J. (1992) *Science 258*, 936−942.
3. Cowan, S. W., Schirmer, T., Rummel, G., Steiert, M., Ghosh, R., Pauptit, R. A., Jansonius, J. N., and Rosenbusch, J. P. (1992) *Nature 358*, 727−733.
4. Phale, P. S., Philippsen, A., Kiefhaber, T., Koebnik, R., Phale, V. P., Schirmer, T., and Rosenbusch, J. P. (1998) *Biochemistry 37*, 15663−15670.
5. Surrey, T., Schmid, A., and Jahnig, F. (1996) *Biochemistry 35*, 2283−228.
6. Kleinschmidt, J. H., and Tamm, L. K. (1999) *Biochemistry 38*, 4996−5005.
7. Kleinschmidt, J. H., den Blaauwen, T., Driessen, A. J., and Tamm, L. K. (1999) *Biochemistry 38*, 5006−5016.
8. Braun, V., and Killmann, H. (1999) *Trends Biol. Sci. 24*, 104−109.
9. Moeck, G. S., and Coulton, J. W. (1998) *Mol. Microbiol. 28*, 675−681.
10. Ferguson, A. D., Hofmann, E., Coulton, J. W., Diederichs, K., and Welte, W. (1998) *Science 282*, 2215−2220.
11. Locher, K. P., Rees, B., Koebnik, R., Mitschler, A., Moulinier, L., Rosenbusch, J. P., and Moras, D. (1998) *Cell 95*, 771−778.
12. Buchanan, S. K., Smith, B. S., Venkatrami, L., Xia, D., Esser, L., Palnitkar, M., Chakraborty, R., van der Helm, D., and Deisenhofer, J. (1999) *Nat. Struct. Biol. 6*, 56−63.
13. Carmel, G., and Coulton, J. W. (1991) *J. Bacteriol. 173*, 4394−4403.
14. Braun, M., Killmann, H., and Braun, V. (1999) *Mol. Microbiol. 33*, 1037−1049.
15. Moeck, G. S., Coulton, J. W., and Postle, K. (1997) *J. Biol. Chem. 272*, 28391−28397.
16. Boulanger, P., Le Maire, M., Bonhivers, M., Dubois, S., Desmadril, M., and Letellier, L. (1996) *Biochemistry 35*, 14216−14224.
17. Moeck, G., Tawa, P., Xiang, H., Ismail, A., Turnbull, J., and Coulton, J. (1996) *Mol. Microbiol. 22*, 459−471.
18. Bonhivers, M., Ghazi, A., Boulanger, P., and Letellier, L. (1996) *EMBO. J. 15*, 1850−1856.
19. Moeck, G. S., Ratcliffe, M. J., and Coulton, J. W. (1995) *J. Bacteriol. 177*, 6118−6125.
20. Dornmair, K., Kiefer, H., and Jahnig, F. (1990) *J. Biol. Chem. 265*, 18907−18911.

21. Ohnishi, S., Kameyama, K., and Takagi, T. (1998) *Biochim. Biophys. Acta 1375*, 101−109.
22. Locher, K. P., and Rosenbusch, J. P. (1997) *Eur. J. Biochem. 247*, 770−775.
23. Feucht, A., Schmid, A., Benz, R., Schwarz, H., and Heller, K. (1990) *J. Biol. Chem. 265*, 18561−18567.
24. Bonhivers, M. (1995), Thèse de l'Université Pierre et Marie Curie, Paris VI.
25. Lambert, O., Plancon, L., Rigaud, J. L., and Letellier, L. (1999) *Mol. Microbiol. 30*, 761−765.
26. Killmann, H., Videnov, G., Jung, G., Schwarz, H., and Braun, V. (1995) *J. Bacteriol. 177*, 694−698.
27. Koebnik, R., and Braun, V. (1993) *J. Bacteriol. 175*, 826−839.
28. Klug, C. S., Su, W., Liu, J., Klebba, P., and Feix, J. B. (1995) *Biochemistry 34*, 14230−14236.
29. Minard, P., Hall, L., Betton, J. M., Missiakas, D., and Yon, J. M. (1989) *Protein Eng. 3*, 55−60.
30. Markovic-Housley, Z., Cooper, A., Lustig, A., Flukiger, K., Stolz, B., and Erni, B. (1994) *Biochemistry 33*, 10977−10984.
31. Nock, S., Grillenbeck, N., Ahmadian, M. R., Ribeiro, S., Kreutzer, R., and Sprinzl, M. (1995) *Eur. J. Biochem. 234*, 132−139.
32. Mayr, E. M., Jaenicke, R., and Glockshuber, R. (1997) *J. Mol. Biol. 269*, 260−269.
33. Gegg, C. V., Bowers, K. E., and Matthews, C. R. (1997) *Protein Sci. 6*, 1885−1892.
34. Hosszu, L. L., Craven, C. J., Parker, M. J., Lorch, M., Spencer, J., Clarke, A. R., and Waltho, J. P. (1997) *Nat. Struct. Biol. 4*, 801−804.

BI001725I